

KU LEUVEN

FACULTY OF SCIENCE
Department of Chemistry

A very cool Title:

An even cooler subtitle

DRAFT

To remove, add ‘final’ to class options

Mauro Gascón Navas

Dissertation presented in partial fulfillment
of the requirements for the degree of
Erasmus Mundus Master of Science in
Theoretical Chemistry and Computational
Modelling

Supervisors:
Prof. Dr. Thomas Jagau
Prof. dr. ir. S. Leader

June 2025



A VERY COOL TITLE:

AN EVEN COOLER SUBTITLE

Mauro GASCÓN NAVAS

Supervisors:

Prof. Dr. Thomas Jagau

Prof. dr. ir. S. Leader

Members of the

Examination Committee:

Prof. dr. ir. The Chairman, chair

Prof. dr. ir. The One

Prof. dr. ir. The Other

Prof. dr. External Jurymember

(Far Away)

Dissertation presented in partial
fulfillment of the requirements for the
degree of Erasmus Mundus Master
of Science in Theoretical Chemistry
and Computational Modelling

June 2025

© 2025 Mauro Gascón Navas
Uitgegeven in eigen beheer, Mauro Gascón Navas, Leuven (Belgium)

Alle rechten voorbehouden. Niets uit deze uitgave mag worden vermenigvuldigd en/of openbaar gemaakt worden door middel van druk, fotokopie, microfilm, elektronisch of op welke andere wijze ook zonder voorafgaande schriftelijke toestemming van de uitgever.

All rights reserved. No part of the publication may be reproduced in any form by print, photoprint, microfilm, electronic or any other means without written permission from the publisher.

Acknowledgements

...

Thank you thank you.

Instructions by the Arenberg Doctoral School:

The scientific abstract should present the most important aims and conclusions of the dissertation in a brief text of ca. 2 pages.



Abstract

...

Instructions by the Arenberg Doctoral School:

The scientific abstract should present the most important aims and conclusions of the dissertation in a brief text of ca. 2 pages.



Beknopte samenvatting

...aaa

Instructions by the Arenberg Doctoral School:

The scientific abstract should present the most important aims and conclusions of the dissertation in a brief text of ca. 2 pages.



List of Abbreviations

MD molecular dynamics. 3



List of Symbols

Θ A nice symbol



Contents

Acknowledgements	i
Abstract	iii
Beknopte samenvatting	v
List of Abbreviations	vii
List of Symbols	ix
Contents	xi
List of Figures	xiii
List of Tables	xv
1 Introduction	3
1.1 Biological Quinones	3
1.2 Exotic Anions	3
2 Theoretical Background	5
2.1 Self Consistent Field Methods	5
2.1.1 Electron Correlation	7
2.1.2 Møller-Plesset Perturbation Theory	7
2.1.3 Density Functional Theory	8
2.1.4 Configuration Interaction	8
2.1.5 Coupled Cluster Theory	9
2.1.6 Second Approximate Coupled Cluster	11
2.2 Equation-of-Motion Methods	11
2.3 Dyson Orbitals	12
2.3.1 EOM-CC2 Dyson Orbitals	13

3 Computational Methods	17
4 Results and Discussion	19
5 This is conclusion	21
6 Manual	23
6.1 Tips and Tricks	23
6.1.1 Joint PhD Dissertation	23
6.1.2 Image on the cover page	23
6.1.3 Table of contents	24
6.1.4 Small ebook size	24
6.2 Settings for TeXstudio	24
6.2.1 Support for TeXstudio structure panel	24
6.2.2 Custom <i>makeindex</i> and <i>makeglossaries</i> commands . . .	25
6.2.3 Custom Build&View and Compile meta-commands . . .	25
6.3 Full cover page	26
A This is myappendix	27
Bibliography	29

List of Figures

1.1	Short caption for Table of Figures	4
2.1	EOM-EA.	12



List of Tables

2.1	Computational scaling of quantum chemistry methods.	10
-----	---	----



LIST OF TABLES 1

Instructions by the Arenberg Doctoral School:

Report and discussion of the research in different chapters: These chapters, reporting and discussing research results, can be based on text that has already been published or accepted or submitted to journals or conferences. In that case, the bibliographic reference of the publication should be mentioned on the first page of the chapter. If there are multiple authors, the PhD researcher must clarify the own scientific contribution after that bibliographic reference on the first page of the chapter. There is no problem in editing or rewriting a text that has already been published or accepted for publication, for example to reach consistency and coherence in writing style and formatting, to add details that were left out from publication, to meet comments of the Examination Committee, etc; The doctoral candidate must determine whether the publisher allows public availability of the publications and in which form via the webpage Romeo/Sherpa.

Consistency in layout is required for the entire manuscript! References to figures, tables, appendices, and similar structures need to be consistent.



Chapter 1

Introduction

Instructions by the Arenberg Doctoral School:

An in-depth introduction outlining the research in a broader context: Starting from a description of the state of the art in the domain, additionally, the research questions and objectives are formulated. Furthermore, this includes the global approach and research methods.

1.1 Biological Quinones

1.2 Exotic Anions

Illustration of how to include citations [2] and [3]. Lorem ipsum dolor sit amet, consetetur sadipscing elitr, sed diam nonumy eirmod tempor invidunt ut labore et dolore magna aliquyam erat, sed diam voluptua. At vero eos et accusam et justo duo dolores et ea rebum. Stet clita kasd gubergren, no sea takimata sanctus est Lorem ipsum dolor sit amet.

And yet another citation [1].

Introducing some symbol: Θ .

Introducing an acronym: MD.

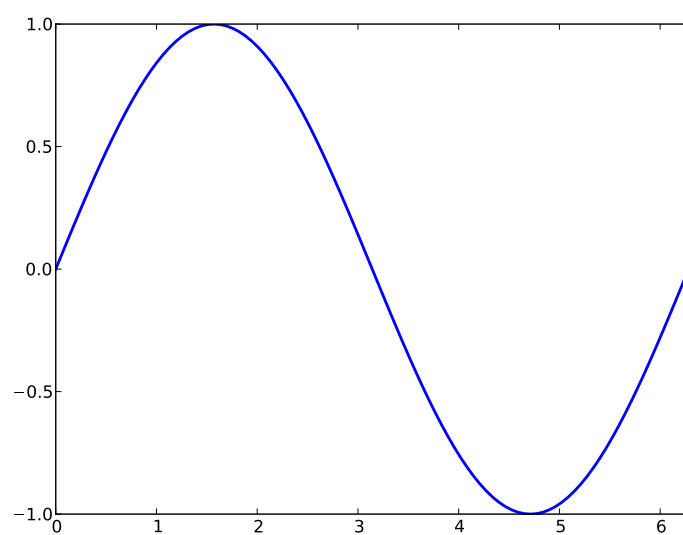


Figure 1.1: Illustration of how to include a figure (long text, should not go to Table of Figures).

Chapter 2

Theoretical Background

2.1 Self Consistent Field Methods

The objective of any quantum chemical calculation is to solve the time-independent Schrödinger equation (TISE) for a many-electron system:

$$\hat{H}\Psi = E\Psi \quad (2.1)$$

However, solving the TISE exactly for systems with more than one electron is computationally infeasible due to the complexity of electron-electron interactions. To address this, approximate methods such as the Hartree-Fock (HF) method have been developed.

The Hartree-Fock (HF) method stands as the cornerstone electronic structure calculations. Its primary objective is to provide an approximate solution to the many-electron time-independent Schrödinger equation within the Born-Openheimer approximation, which governs the behavior of electrons within atoms and molecules: The HF method achieves this by assuming that each electron moves independently within an average electrostatic field generated by the other electrons in the system. In the HF method the N -electron wavefunction is represented by a Slater determinant, which is formed by taking the antisymmetrized product of N individual one-electron spin-orbitals (χ):

$$\Psi(\mathbf{r}_1, \mathbf{r}_2, \dots, \mathbf{r}_N) = \frac{1}{\sqrt{N!}} \begin{vmatrix} \chi_1(\mathbf{r}_1) & \chi_2(\mathbf{r}_1) & \cdots & \chi_N(\mathbf{r}_1) \\ \chi_1(\mathbf{r}_2) & \chi_2(\mathbf{r}_2) & \cdots & \chi_N(\mathbf{r}_2) \\ \vdots & \vdots & \ddots & \vdots \\ \chi_1(\mathbf{r}_N) & \chi_2(\mathbf{r}_N) & \cdots & \chi_N(\mathbf{r}_N) \end{vmatrix} \quad (2.2)$$

The choice of using a determinant inherently satisfies both the Pauli exclusion principle, and the antisymmetry requirement of fermions. The energy expectation for a Slater determinant according to HF is variational and can be computed as:

$$\begin{aligned}
 E_{HF} &= \langle \Psi | \sum_{i=1}^N \hat{F}_i | \Psi \rangle \\
 &= \langle \Psi | \sum_{i=1}^N \hat{h}(i) + \sum_{i,j=1}^N (2\hat{J}_j(i) - \hat{K}_j(i)) | \Psi \rangle \\
 &= \sum_{i=1}^N \langle \chi_i | \hat{h} | \chi_i \rangle + \frac{1}{2} \sum_{i,j=1}^N \langle \chi_i \chi_j | | \chi_i \chi_j \rangle
 \end{aligned} \tag{2.3}$$

Where, \hat{F} is the Fock operator. \hat{F} is made up from \hat{h} , the one-electron core Hamiltonian operator (kinetic energy and electron-nucleus attraction); $\hat{J}_j(i)$, the Coulomb operator, describing the electrostatic repulsion between electron i and the average charge distribution of electron j , and $\hat{K}_j(i)$ is the exchange operator, a purely quantum mechanical term arising from the antisymmetry principle. Because of the two electron terms, the computational cost of HF scales as $O(N^4)$.

The Hartree-Fock equations are inherently non-linear: because the Fock operator depends on the wavefunctions of all the other electrons, their interactions are coupled. Consequently, these equations cannot be solved analytically and are solved using an iterative procedure known as the self-consistent field (SCF) method, where the final field experienced by the electrons must be consistent with the electron distribution that generates that field. The SCF procedure involves the following steps: An initial guess for the spin-orbitals is made. Using this initial guess, the Fock operator is constructed. The Hartree-Fock equations are then solved by diagonalizing the Fock operator to obtain a new set of molecular orbitals and their corresponding energies. This new set of orbitals is compared to the previous set. If the change is below a predefined threshold, the procedure is considered converged, and the SCF is achieved. If convergence is not reached, the new set of orbitals is used to construct a new Fock operator, and the process is repeated. Convergence signifies that a stable electronic configuration has been reached within the limitations of the Hartree-Fock approximation.

In practical Hartree-Fock calculations, the spinorbitals are expressed as linear combinations of predefined mathematical functions known as basis functions. The set of these functions is called a basis set. Because a finite basis set cannot exactly represent the spinorbitals, they greatly define the level of accuracy

and computational cost of the calculation. Larger basis sets generally lead to more accurate descriptions of the electronic structure at the cost of increased computational effort.

2.1.1 Electron Correlation

The Hartree-Fock (HF) method is inherently limited by its neglect of the instantaneous interactions of electrons. In the HF approximation, each electron is treated as moving independently within a static, average field created by the other electrons. This mean-field approach fails to account for the fact that electrons will instantaneously repel each other, leading to a correlated movements as they try to avoid each other in space.

The primary consequence of neglecting electron correlation in the HF approximation is an overestimation of the electron-electron repulsion energy. While the HF method does account for the exchange interaction exactly as a consequence of the antisymmetry of the Slater determinant (Fermi correlation), it completely neglects the Coulomb, or dynamic, correlation. This omission leads to a higher electronic energy than the exact solution, and an inability to accurately predict certain phenomena, such as London dispersion forces.

The difference between the exact non-relativistic energy of the system and the energy obtained in the HF complete basis limit is defined as the correlation energy and is always negative due to the variational principle. Correlated methods aim to include the effects of the instantaneous interactions between electrons that are neglected in the mean-field approximation of HF theory. In the following sections, several correlated methods relevant to this work are presented.

2.1.2 Møller-Plesset Perturbation Theory

Møller-Plesset (MP) perturbation theory offers a way to improve upon the HF energy by the use of Raylei-Schro perturbation theory: the electron correlation is treated as a perturbation to the HF Hamiltonian. The energy and wavefunction are then expanded as a series in terms of the perturbation strength. The first-order energy correction in MP theory is zero, so the first non-trivial correction to the HF energy appears at the second order, giving rise to the MP2 method. The MP2 energy correction for a closed-shell molecule is given by:

$$E_{\text{MP2}} = -\frac{1}{4} \sum_{ij}^{\text{occ}} \sum_{ab}^{\text{virt}} \frac{|\langle ij || ab \rangle|^2}{\epsilon_a + \epsilon_b - \epsilon_i - \epsilon_j} \quad (2.4)$$

Where i, j denote occupied molecular orbitals, a, b denote virtual molecular orbitals, and ϵ are the corresponding orbital energies from the HF calculation. MP theory can be extended to higher orders (MP3, MP4, etc.) to achieve greater accuracy, although the computational cost increases significantly with each order. The computational cost of MP2 scales as $O(N^5)$.

2.1.3 Density Functional Theory

Density Functional Theory (DFT) provides an alternative approach to incorporating electron correlation by parametrizing the energy on the electron density rather than the wavefunction, reducing the degrees of freedom of the system from $3N - 3$ to just 3. In the most commonly used form of DFT, the Kohn-Sham method, the problem is formulated in terms of orbitals that are not physical, but are chosen to reproduce the electron density of the system. The fundamental principle of DFT is that the ground state energy of a system is a unique functional of its electron density:

$$\left(-\frac{1}{2}\nabla^2 + \hat{V}_{\text{ext}}(\mathbf{r}) + \hat{V}_{\text{H}}(\mathbf{r}) + \hat{V}_{\text{XC}}[\rho(\mathbf{r})] \right) \psi_i(\mathbf{r}) = \epsilon_i \psi_i(\mathbf{r}) \quad (2.5)$$

Where \hat{V}_{ext} represents the external potential, $\hat{V}_{\text{H}}(\mathbf{r}) = \int \frac{\rho(\mathbf{r}')}{|\mathbf{r} - \mathbf{r}'|} d\mathbf{r}'$ is the Hartree potential, \hat{V}_{XC} is the Exchange-Correlation potential and $\rho(\mathbf{r})$ is the electron density. The exchange-correlation functional is the most challenging part of DFT, as it is not known exactly and must be approximated. The accuracy of DFT calculations depends heavily on the choice of exchange-correlation functional. The computational cost of DFT scales as $O(N^4)$.

2.1.4 Configuration Interaction

Configuration Interaction (CI) methods improve upon HF by expressing the electronic wavefunction as a linear combination of the HF ground state determinant and excited state determinants:

$$|\Psi_{\text{CI}}\rangle = c_0|\Phi_0\rangle + \sum_{ia} c_{ia}|\Phi_{ia}\rangle + \sum_{ijab} c_{ijab}|\Phi_{ijab}\rangle + \dots \quad (2.6)$$

Where $|\Phi_0\rangle$ is the HF ground state determinant, $|\Phi_{ia}\rangle$ represents a determinant with a hole in spin-orbital i and a particle in the spin-orbital a , and c are the CI coefficients. Full CI (FCI), includes all possible excitations within a given one-electron basis set and represents the exact solution to the non-relativistic Schrödinger equation in that basis. However, is computationally prohibitive

for all but the simplest systems. Full Configuration Interaction (FCI) includes all possible excitations within a given one-electron basis set and represents the exact solution to the non-relativistic Schrödinger equation in that basis. However, it is computationally prohibitive for all but the simplest systems. Truncated CI methods, such as CISD (singles and doubles), are more practical but lack size extensivity — a property ensuring that the energy of a system scales correctly with the number of non-interacting subsystems. A method is size-extensive if, for two infinitely separated molecules A and B , the total energy satisfies $E(A + B) = E(A) + E(B)$. Truncated CI methods fail to satisfy this condition because they do not include all necessary higher-order excitations, leading to an underestimation of the total energy as system size grows. CI are, however, size-consistent, meaning that the energy behaviour remains consistent when interaction between the involved molecular subsystems is nullified (by distance, for instance). While CISD is size-consistent, its lack of size extensivity makes it unsuitable for extensive systems.

2.1.5 Coupled Cluster Theory

Similarly to CI, the coupled cluster CC method expands the wavefunction as a linear combination of Slater determinants. However, the CC wavefunction is size-extensive and size-consistent by using an exponential ansatz,

$$|\Psi_{CC}\rangle = e^{\hat{T}}|\Psi_0\rangle \quad (2.7)$$

where \hat{T} is the cluster operator, which is the central component of CC theory and is defined as a sum of excitation operators,

$$\hat{T} = \hat{T}_1 + \hat{T}_2 + \hat{T}_3 + \cdots + \hat{T}_N \quad (2.8)$$

where N is the total number of electrons in the system. Each term in this sum corresponds to a specific level of excitation and is expressed within the second quantization formalism:

- $\hat{T}_1 = \sum_i^{\text{occ}} \sum_a^{\text{virt}} t_i^a a_a^\dagger a_i$ represents single excitations.
- $\hat{T}_2 = \frac{1}{4} \sum_{i,j}^{\text{occ}} \sum_{a,b}^{\text{virt}} t_{ij}^{ab} a_a^\dagger a_b^\dagger a_j a_i$ represents double, *coupled* excitations.
- Higher-order excitation operators $\hat{T}_3, \hat{T}_4, \dots$ describe coupled excitation of three, four, and more electrons, respectively.

The coefficients t_i^a , t_{ij}^{ab} , etc., are cluster amplitudes to be determined by projection of the CC Schrödinger equation onto the excited determinant. The exponential

form, expanded as a Taylor series,

$$e^{\hat{T}} = 1 + \hat{T} + \frac{1}{2!}\hat{T}^2 + \dots \quad (2.9)$$

inherently includes terms that represent disconnected clusters, which ensures for size consistency. The energy is obtained by projecting onto the HF reference determinant:

$$E_{\text{CC}} = \langle \Psi_0 | e^{-\hat{T}} \hat{H} e^{\hat{T}} | \Psi_0 \rangle \quad (2.10)$$

Using the Baker-Campbell-Hausdorff expansion, the exponential operators in Eq. 2.10 can be simplified to a series of commutators which ends at the fourth order. The cluster operator \hat{T} can be truncated at different levels of excitation:

- **CCD** (Coupled Cluster Doubles): This is the simplest approximation in the CC family, where the cluster operator is truncated to include only double excitations: $\hat{T} \approx \hat{T}_2$. There is no CC Singles since the Brillouin’s theorem implies that the amplitudes of single excitations alone are null.
- **CCSD** (Coupled Cluster Singles and Doubles): This is one of the most widely used and generally accurate *ab initio* methods, where the cluster operator includes both single and double excitations: $\hat{T} \approx \hat{T}_1 + \hat{T}_2$.
- **CCSDT** (Coupled Cluster Singles, Doubles, and Triples): $\hat{T} \approx \hat{T}_1 + \hat{T}_2 + \hat{T}_3$.
- ...

The hierarchy can be extended to include even higher levels of excitation, with the properties converging to the FCI limit. The computational cost of CC methods increases rapidly with the level of truncation, as shown in Table 2.1.

Method	Operation count	Memory
HF	$O(N^4)$	$O(N^4)$
MP2	$O(N^5)$	$O(N^4)$
CCD/CCSD	$O(N^6)$	$O(N^4)$
CCSDT	$O(N^8)$	$O(N^6)$
CC2	$O(N^5)$	$O(N^4)$

Table 2.1: Computational scaling of quantum chemistry methods.

2.1.6 Second Approximate Coupled Cluster

Second Approximate Coupled Cluster (CC2) belongs to the broader family of CCn approximate coupled cluster methods, where the ‘n’ in CCn indicates the truncation of the cluster operator within a perturbative hierarchy. These methods aim to reduce the computational cost associated with standard CC truncations while still retaining a reasonable level of accuracy.

In CC2, the equations for the single amplitudes, t_i^a , are the same as CC theory (Eq. 2.7) under the constraint that the doubles amplitudes, t_{ij}^{ab} , are calculated using the non-iterative expression for MP2 (Eq 2.4). The resulting expression for the CC2 correlation energy is:

$$E_{CC2} = \sum_{ij}^{\text{occ}} \sum_{ab}^{\text{virt}} \frac{1}{4} \frac{|\langle ij || ab \rangle|^2}{\epsilon_a + \epsilon_b - \epsilon_i - \epsilon_j} + \sum_i^{\text{occ}} \sum_a^{\text{virt}} \hat{F}_{ai} t_i^a \quad (2.11)$$

The perturbative treatment of the doubles amplitudes in CC2, reduces the computational cost compared to CCSD, Table 2.1. While this approximation can lead to a less accurate description of electron correlation, the inclusion of singles amplitudes allows for an approximate description of orbital relaxation, which often leads to higher quality wavefunction, and hence properties, compared to MP2.

2.2 Equation-of-Motion Methods

Equation-of-Motion Coupled Cluster (EOM-CC) methods are an extension of ground-state coupled cluster theory which provide a framework for calculating a variety of excited (EE), ionized (IP) and electron-attached (EA) states. In the EOM-CC, the target electronic state is generated by applying a linear excitation operator \hat{R} to a reference state, which typically is the coupled cluster wavefunction of the ground state. The target state wavefunction can then be expressed as $|\Psi_{\text{EOM}}\rangle = \hat{R}|\Psi_{\text{CC}}\rangle = \hat{R}e^{\hat{T}}|\Phi_{\text{HF}}\rangle$. Figure 2.1, shows some of the determinats of $|\Psi_{\text{EA}}\rangle$, where the target state has one more α electron.

The form of the operator \hat{R} is similar to the cluster operator and chosen to access the desired target state. In the case of EOM-EA, the electron attachment operator R^{EA} includes terms that describe the creation of one electron to an unoccupied orbital, terms that describe the creation of one electron accompanied by the excitation of another electron from an occupied to an unoccupied orbital,

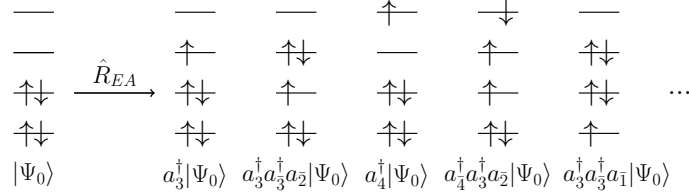


Figure 2.1: EOM-EA.

and so on:

$$\hat{R}^{\text{EA}} = \hat{R}_1^{\text{EA}} + \hat{R}_2^{\text{EA}} + \dots = \sum_a r^a a_a^\dagger + \frac{1}{2} \sum_{ab} \sum_i r_i^{ba} a_b^\dagger a_a^\dagger a_i + \dots \quad (2.12)$$

Where a and b denote virtual orbitals, i denotes an occupied orbital, and r^a and r_i^{ba} are the coefficients to be determined. By truncating at the same excitation level as the cluster operator, the method is rigorously size-extensive and size-consistent. The EA energies, or any other EOM energy, can be obtained as the eigenvalues of the similarity-transformed Hamiltonian, \bar{H}_N :

$$\bar{H}_N \hat{R} |\Psi_0\rangle = \Delta E_{\text{EOM}} \hat{R} |\Psi_0\rangle \quad (2.13)$$

$$\bar{H}_N = e^{-\hat{T}} \hat{H} e^{\hat{T}} - \langle \Psi_0 | e^{-\hat{T}} \hat{H} e^{\hat{T}} | \Psi_0 \rangle \quad (2.14)$$

Since the similarity transformed hamiltonian is non-hermitian, the left and right are different but correspond to the same eigenvalues. This means that the properties have ‘right’ and ‘left’ expectation values.

The strength of the EOM-CC ansatz is the use of a closed shell reference to access open shell states, which are eigenfunctions of the \hat{S}^2 operator. The EOM-CC methods are also size-extensive and size-consistent. The computational cost of EOM-CC methods is similar to that of the corresponding ground-state CC methods.

2.3 Dyson Orbitals

Dyson orbitals are defined as the overlap between the wavefunction of an initial N -electron state ($|\Psi_0^N\rangle$) and the wavefunction of the final state with $N \pm 1$ electrons ($|\Psi_f^{N \pm 1}\rangle$).

$$\phi_d(r_1) = \sqrt{N} \int \Psi^N(r_2, \dots, r_N) \Psi^{N+1}(r_1, r_2, \dots, r_N) dr_2 \dots dr_N \quad (2.15)$$

Because the the terms differ in one electron, the result of the overlap is a vector instead of a scalar, and can be expressed as a linear combination of the molecular orbitals ($\phi_p(r)$) of the reference wavefunction:

$$\phi_d(r) = \sum_p \gamma_p \phi_p(r) \quad (2.16)$$

where γ_p are the coefficients that quantify the contribution of each molecular orbital to the Dyson orbital. Physically, Dyson orbitals can be interpreted as the correlated analog to the orbital of the electron that is either removed or attached.

The norm squared of the Dyson orbital, (P), is calculated by integrating the squared modulus of the Dyson orbital over all space:

$$P = \int |\phi_{Dyson}(r)|^2 dr = \sum_{p,q} \gamma_p^* \gamma_q \langle \phi_p | \phi_q \rangle \quad (2.17)$$

The pole strength ranges from 0 to 1 and provides a direct measure of the one-electron character of the ionization or electron attachment process. As the open shell wavefunction is usually obtained by means of a EOM-CC method, there are a ‘left’ and ‘right’ Dyson orbital.

They can be used for the interpretation and prediction of photoelectron spectra as they contain all the information required to calculate differential cross-sections, $\frac{d\sigma}{d\Omega_k}$:

$$\frac{d\sigma}{d\Omega_k} = \frac{4\pi^2 k E}{c} |\langle \phi_d | \mu | \Psi_k^{el} \rangle|^2 \quad (2.18)$$

where where k is the magnitude of the photoelectron wavevector, E is the energy of the ionizing radiation, and c is the speed of light, μ is the dipole operator, and Ψ_k^{el} is the photoelectron wavefunction, and a strong orthonormality is assumed between the reference and continuum wavefunction.

2.3.1 EOM-CC2 Dyson Orbitals

Computes O block of matrix elements of dyson orbitals using CC and EOM-EA wave functions:

$$\langle EA | a | EE \rangle = \langle 0 | L^{EE} (a e^T)_c R^{EA} | 0 \rangle$$

The storage convention assumed for the r2 IP amplitudes is:

$$r2_{ij}^a a^\dagger j i - - - r2(i|j|a)$$

The storage convention assumed for the l2 IP amplitudes is

$$l2_{ij}^a i^\dagger j^\dagger a - - - l2(i|j|a)$$

EOM-EA-Dyson Equations

Right Dyson orbital, $\phi_D^{\text{EA},\text{R}} = \sum_i^{\text{occ}} \gamma_i^{\text{EA},\text{R}} \phi_i + \sum_a^{\text{vir}} \gamma_a^{\text{EA},\text{R}} \phi_a$:

$$\begin{aligned} \gamma_i^{\text{EA},\text{R}} &= \langle EA | a_i^\dagger | CC \rangle = \langle 0 | L^{EA} (a^\dagger e^T)_c | 0 \rangle \\ &= - \sum_c t_{ic} l_c - \frac{1}{2} \sum_{kcd} t_{ki}^{dc} l_{dc}^k \end{aligned} \quad (2.19)$$

$$\begin{aligned} \gamma_a^{\text{EA},\text{R}} &= \langle EA | a_a^\dagger | CC \rangle \\ &= l_a \end{aligned} \quad (2.20)$$

Left Dyson orbital, $\phi_D^{\text{EA},\text{L}} = \sum_i^{\text{occ}} \gamma_i^{\text{EA},\text{L}} \phi_i + \sum_a^{\text{vir}} \gamma_a^{\text{EA},\text{L}} \phi_a$:

$$\begin{aligned} \gamma_i^{\text{EA},\text{L}} &= \langle CC | a_i | EA \rangle \\ &= - \sum_c \lambda_{ic} r_c - \frac{1}{2} \sum_{kcd} \lambda_{ik}^{cd} r_k^{dc} \end{aligned} \quad (2.21)$$

$$\begin{aligned} \gamma_a^{\text{EA},\text{L}} &= \langle CC | a_a | EA \rangle \\ &= r_a + \sum_{kc} \lambda_{kc} r_{ca}^k + \sum_k \gamma_k^{\text{EA},\text{L}} t_{ka} - \frac{1}{2} \sum_{klcd} \lambda_{lk}^{dc} l_{lk}^{da} r_c \end{aligned} \quad (2.22)$$

EOM-EA-EE-Dyson Equations

Right Dyson orbital, $\phi_D^{\text{EA-EE},\text{R}} = \sum_i^{\text{occ}} \gamma_i^{\text{EA-EE},\text{R}} \phi_i + \sum_a^{\text{vir}} \gamma_a^{\text{EA-EE},\text{R}} \phi_a$:

$$\begin{aligned} \gamma_i^{\text{EA-EE},\text{R}} &= \langle EA | a_i^\dagger | EE \rangle \\ &= r_0 \gamma_a^{\text{EA},\text{R}} - \sum_c r_{ic} l_c - \frac{1}{2} \sum_{lcd} r_{il}^{cd} l_{dc}^l - \sum_{lcd} l_{dc}^l t_{ic} r_{ld} \end{aligned} \quad (2.23)$$

$$\begin{aligned} \gamma_a^{\text{EE-EA},\text{R}} &= \langle EA | a_a^\dagger | EE \rangle \\ &= r_0 l_a + \sum_{kc} l_{ca}^k r_{kc} \end{aligned} \quad (2.24)$$

Left Dyson orbital, $\phi_D^{\text{EE-EA,L}} = \sum_i^{\text{occ}} \gamma_i^{\text{EE-EA,L}} \phi_i + \sum_a^{\text{vir}} \gamma_a^{\text{EE-EA,L}} \phi_a$:

$$\begin{aligned} \gamma_i^{\text{EE-EA,L}} &= \langle EE | a_i | EA \rangle \\ &= - \sum_c l_{ic} r_c - \frac{1}{2} \sum_{kcd} l_{ik}^{cd} r_k^{dc} \end{aligned} \quad (2.25)$$

$$\begin{aligned} \gamma_a^{\text{EE-EA,L}} &= \langle EE | a_a | EA \rangle \\ &= \sum_{kc} l_{kc} r_{ca}^k + \sum_k \gamma_k^{\text{EE-EA,L}} t_{ka} - \frac{1}{2} \sum_{klcd} l_{lk}^{dc} t_{lk}^{da} r_c \end{aligned} \quad (2.26)$$

EOM-IP-Dyson Equations

Right Dyson orbital, $\phi_D^{\text{EE,R}} = \sum_i^{\text{occ}} \gamma_i^{\text{IP,R}} \phi_i + \sum_a^{\text{vir}} \gamma_a^{\text{IP,R}} \phi_a$:

$$\begin{aligned} \gamma_a^{\text{IP,R}} &= \langle CC | a_a^\dagger | IP \rangle \\ &= \lambda_{ka} r_k + \frac{1}{2} \lambda_{lk}^{ca} r_{klc} \end{aligned} \quad (2.27)$$

$$\begin{aligned} \gamma_i^{\text{IP,R}} &= \langle CC | a_i^\dagger | IP \rangle \\ &= r_i + \sum_{kc} \lambda_{kc} r_{ik}^c - \sum_c \gamma_c^{\text{IP,R}} t_{ic} - \frac{1}{2} \sum_{klcd} \lambda_{lk}^{dc} t_{li}^{dc} r_k \end{aligned} \quad (2.28)$$

Left Dyson orbital, $\phi_D^{\text{IP,L}} = \sum_i^{\text{occ}} \gamma_i^{\text{IP,L}} \phi_i + \sum_a^{\text{vir}} \gamma_a^{\text{IP,L}} \phi_a$:

$$\begin{aligned} \gamma_i^{\text{IP,L}} &= \langle IP | a_i | CC \rangle \\ &= l_i \end{aligned} \quad (2.29)$$

$$\begin{aligned} \gamma_a^{\text{IP,L}} &= \langle IP | a_a | CC \rangle \\ &= \sum_k t_{ka} l_k + \frac{1}{2} \sum_{klc} t_{kl}^{ac} l_{kl}^c \end{aligned} \quad (2.30)$$

EOM-EE-IP-Dyson Equations

Right Dyson orbital, $\phi_D^{\text{EE-IP,R}} = \sum_i^{\text{occ}} \gamma_i^{\text{EE-IP,R}} \phi_i + \sum_a^{\text{vir}} \gamma_a^{\text{EE-IP,R}} \phi_a$:

$$\begin{aligned}\gamma_i^{\text{EE-IP,R}} &= \langle EE|a_i^\dagger|IP\rangle \\ &= \sum_{kc} l_{kc} r_{ik}^c - \sum_c \gamma_c^{\text{IP-EI}} t_{ic} - \frac{1}{2} \sum_{klcd} l_{lk}^{dc} t_{li}^{dc} r_k\end{aligned}\quad (2.31)$$

$$\begin{aligned}\gamma_a^{\text{EE-IP,R}} &= \langle EE|a_a^\dagger|IP\rangle \\ &= l_{ka} r_k + \frac{1}{2} l_{lk}^{ca} r_{klc}\end{aligned}\quad (2.32)$$

Left Dyson orbital, $\phi_D^{\text{IP-EE,L}} = \sum_i^{\text{occ}} \gamma_i^{\text{IP-EE,L}} \phi_i + \sum_a^{\text{vir}} \gamma_a^{\text{IP-EE,L}} \phi_a$:

$$\begin{aligned}\gamma_i^{\text{IP-EE,L}} &= \langle IP|a_i|EE\rangle \\ &= r_0 l_i + \sum_{kc} l_{ik}^c r_{kc}\end{aligned}\quad (2.33)$$

$$\begin{aligned}\gamma_a^{\text{IP-EE,L}} &= \langle IP|a_a|EE\rangle \\ &= r_0 \gamma_a^{\text{IP,L}} + \sum_k r_{ka} l_k + \frac{1}{2} \sum_{klc} r_{kl}^{ac} l_{kl}^c + \sum_{klc} l_{kl}^c t_{ka} r_{cl}\end{aligned}\quad (2.34)$$

Chapter 3

Computational Methods

...

This are my methods

Instructions by the Arenberg Doctoral School:

Appendices: The appendices should include parts of the research which are essential for the work, but which may hamper the readability of the text, e.g. because of their length (mathematical deductions, experimental data, examples, figures, etc.).



Chapter 4

Results and Discussion

...



Chapter 5

This is conclusion

...

Instructions by the Arenberg Doctoral School:

An extensive conclusion, including a global discussion of the research results, a discussion of the implications of the PhD research and future perspectives in regards to follow-up research.



Chapter 6

Manual

6.1 Tips and Tricks

6.1.1 Joint PhD Dissertation

Add the `joint` option to the document class, change the `PARTNER_LOGO.eps` file and fill in the commands such as `\facultypartner` in `thesis.tex`.

6.1.2 Image on the cover page

If you want to place an image on the cover of the dissertation, you can add the code underneath to the template (check with your promotor whether this is allowed).

Include image: Search for the `\frontcoverheaderXXIV` command in the `adsphd.cls` file and add the following lines:

```
\begin{textblock*}{56mm}(10mm+#1,15mm)
\includegraphics[width=56mm,height=20mm]{image/filename}
\end{textblock*}
```

Where 56mm is the width, 20mm the height, 10mm the x-location and 15mm the y-location.

Change cover font color: Add the command `\color{red}` to the `\frontcoverheaderXXIV` command or enclose specific parts. For example, `{\color{red}\textbf{\@authorf\@author1}}`.

6.1.3 Table of contents

To remove list of figures, tables and other preface chapters from the table of contents, search for occurrences of `\addcontentsline` in the file `adsphd.cls` and comment them.

6.1.4 Small ebook size

When you add the `epub` option to the `adsphd` class the dissertation is printed to a smaller size to read on a device such as Kindle.

Environments such as tables or `tikZ` pictures are often sized in absolute values and not relative to the size of the output. You can wrap them in a `resizebox` to enforce scaling:

```
\resizebox{\textwidth}{!}{%
  \begin{tabular}{cc}
    ...
  \end{tabular}
}
```

6.2 Settings for TeXstudio

If you are working with TeXstudio or other windows latex editors you might want to adjust the editor’s settings to allow a proper compilation of the table of contents and list of figures/tables.

6.2.1 Support for TeXstudio structure panel

The chapters do not show up in the TeXstudio structure panel because the `\includechapter` is not recognized. You can replace this command with the following two lines in `thesis.tex` (replace `manual` with the chapter name):

```
% \includechapter{manual}
```

```
\graphicspath{{chapters/manual/image/}}%
\include{chapters/manual/manual}%
```

6.2.2 Custom *makeindex* and *makeglossaries* commands

According to the *README.md* the tables are indexed through two custom commands. To edit them in TeXstudio open the *Commands* settings (*Options* → *Configure TeXstudio...*, *Commands* sheet), edit the following fields and press OK.

Makeindex:

```
"C:/Program Files/MiKTeX 2.9/miktex/bin/x64/makeindex.exe" %.nlo -s nomencl.ist -o %.nls
```

Makeglossaries:

```
"C:/Program Files/MiKTeX 2.9/miktex/bin/x64/makeindex.exe" %.glo -s %.ist -t %.glg -o %.gls
```

Now the customized commands can be launched by using *Tools* → *Commands* → *MakeIndex/Makeglossaries*. If you want to automatize it in the standard *Build & View* (F5) and *Compile* (F6) commands look at the following section.

6.2.3 Custom Build&View and Compile meta-commands

Open *Options* → *Configure TeXstudio...*, *Build* sheet, edit the following field and press OK.

Build & View:

```
txs:///pdflatex | txs:///bibtex | txs:///makeglossaries | txs:///makeindex |
txs:///pdflatex | txs:///pdflatex
```

To view the PDF once created you have to press F7 (or *Tool* → *View*) and the PDF will automatically update in the default viewer when you modify it.

If you prefer to directly view the created PDF **from the beginning** edit the field as follow:

```
txs:///pdflatex | txs:///bibtex | txs:///makeglossaries | txs:///makeindex |
txs:///pdflatex | txs:///pdflatex | txs:///view-pdf
```

6.3 Full cover page

Important: most printing services will create their own cover page based on the details you send them (title, name, affiliation, ...) and do not supply you with all necessary parameters (e.g., thickness of the paper) because these differ from machine to machine. Therefore, the generated cover page is only indicative and probably not used by your printing server (or even correct).

A full cover page (combining front cover, spine and back cover) can be generated automatically using the command `make cover` or `python3 run.py cover`. This creates a pdf `$(COVERPDF)`; by default this is `cover.pdf`.

The width of the spine is set by redefining `adsphdspinewidth` (9mm by default).

It can be seen in the provided `thesis.tex` that all information necessary to generate a cover page is contained between two markers

```
%%% COVER: Settings %%%
...
%%% COVER: End settings %%%
```

DO NOT REMOVE THESE!! They are used by the Makefile!!

The default front and/or back cover page can be overwritten:

- create a file `mycoverpage.tex`
- redefine the commands `\makefrontcovergeneral` and `\makebackcovergeneral`. For an example and more information, see the provided file `mycoverpage.tex`.

The cover page in the generated pdf has the following structure:

```
<--rbleed--><--backcoverpage--><--lbleed--><--spine width--><--lbleed--><--frontcoverpage--><--rbleed-->
```

The default bleed (both lbleed and rbleed) is 7mm. I suggest not changing this value unless you know what you are doing ;) The latter can be done by redefining `\defaultlbleed` and `\defaultlbleed` respectively.

Appendix A

This is myappendix

...

Instructions by the Arenberg Doctoral School:

Appendices: The appendices should include parts of the research which are essential for the work, but which may hamper the readability of the text, e.g. because of their length (mathematical deductions, experimental data, examples, figures, etc.).



Bibliography

- [1] FREDERIX, Y., AND ROOSE, D. A drift-filtered approach to diffusion estimation for multiscale processes. In *Coping with complexity: model reduction and data analysis* (2010), vol. 75 of *Lecture Notes in Computational Science and Engineering*, Springer-Verlag.
- [2] MEERT, W. *Inference and Learning for Directed Probabilistic Logic Models*. PhD thesis, Informatics Section, Department of Computer Science, Faculty of Engineering, Mar. 2011. Blockeel, Hendrik (supervisor).
- [3] VAN DEN BROECK, G., TAGHIPOUR, N., MEERT, W., DAVIS, J., AND DE RAEDT, L. Lifted probabilistic inference by first-order knowledge compilation. In *Proceedings of the 22th International Joint Conference on Artificial Intelligence (IJCAI)* (2011).

Instructions by the Arenberg Doctoral School:

Bibliography: Should be arranged according to the guidelines generally accepted in the relevant research domain.

The thesis needs to be consistent in relation to bibliographic and other references. Either a global list of bibliographic references is provided at the end of the thesis, or each chapter contains bibliographic references at the end, but there cannot be a combination of these two methods of referencing.

Statement on the use of Generative AI

Instructions by the Arenberg Doctoral School:

Read the guidelines in relation to GenAI at KU Leuven and add the ‘statement on the use of Generative AI’ in your manuscript.

Uncomment the appropriate sentences in the `\useOfGenAI` command and expand the text where needed to make it more specific and add topics if they are not covered by any of the indicated topics.

The text, code, and images in this thesis are my own (unless otherwise specified). Generative AI has only been used in accordance with the KU Leuven guidelines and appropriate references have been added. I have reviewed and edited the content as needed and I take full responsibility for the content of the thesis.

List of publications

Input file chapters/publications/publications.tex does not exist. Make sure its starts with “\chapter{List of publications}”. To not include this chapter in the table of contents, use the starred version of the \chapter command. . .

Instructions by the Arenberg Doctoral School:

List of scientific publications with a clear DOI (digital object identifier) number mentioned:(optional): The list of scientific publications by the doctoral researcher should be arranged according to the guidelines generally accepted in the relevant research domain.





DEPARTMENT OF CHEMISTRY
DEPARTMENT OF CHEMISTRY
Celestijnenlaan 200A box 2402
B-3001 Leuven
first.name@dept.kuleuven.be
<https://chem.kuleuven.be/en/research/qcpc/tue/>

